Graphene-based voltage-tunable coherent terahertz emitter

S. A. Mikhailov*
Institute of Physics, University of Augsburg, D-86135 Augsburg, Germany
(Received 9 August 2012; revised manuscript received 21 December 2012; published 7 March 2013)

A portion of the electromagnetic wave spectrum between ∼0.1 and ∼10 terahertz (THz) suffers from the lack of powerful, effective, easy-to-use, and inexpensive emitters, detectors, and mixers. We propose a multilayer graphene—boron-nitride heterostructure which is able to emit radiation in the frequency range ∼0.1–30 THz with the power density up to ∼0.5 W/cm^2 at room temperature. The proposed device is extremely thin, light, flexible, almost invisible, and may become an important member of the family of devices operating at terahertz frequencies.

DOI: 10.1103/PhysRevB.87.115405 PACS number(s): 78.67.Wj, 78.45.+h, 41.60.−m

I. INTRODUCTION

If a fast electron moves in a periodic potential $U(x) \sim \sin(2\pi x/a_x)$ with the average (nonrelativistic) velocity v_0, its momentum p_x, as well as velocity $v_x = p_x/m$, oscillates in time with the frequency,

$$f = \frac{v_0}{a_x}. \tag{1}$$

Since electrons are charged particles, such oscillations are accompanied by electromagnetic radiation with the frequency (1) (Ref. 1). This physical principle is used in backward-wave oscillators and free-electron lasers, where the potential $U(x)$ is produced by periodic in space electric or magnetic fields. The frequency of radiation can be tuned in these devices by varying the accelerating voltage which determines the electron velocity v_0.

It was a long dream of scientists to create a compact solid-state emitter operating on the same physical principle. Numerous attempts have been made[2–12] to get the coherent Smith-Purcell radiation from semiconductor heterostructures (e.g., GaAs quantum wells) with two-dimensional (2D) electrons: Placing a metallic grating in the vicinity of the 2D conducting layer and driving electrons across the grating stripes it seemed to be possible to force all electrons to emit electromagnetic waves at the frequency (1). However, instead of the strong coherent emission at the frequency (1) a weak incoherent (thermal) radiation at the frequency of two-dimensional plasmons,

$$f_p = \sqrt{\frac{n_s e^2}{m^\star \epsilon a_x}}, \tag{2}$$

was observed in such experiments (see recent reviews[11,12] and references therein); here e, $m^\star$, and n_s are the charge, the effective mass, and the surface density of 2D electrons and ϵ the dielectric constant of the surrounding medium.

The reason for such behavior of semiconductor emitters was explained in Ref. 13. It was shown that the single-particle formula (1) is valid only at $f_p \ll v_0/a_x$, i.e., if the density of electrons is sufficiently low and the drift velocity v_0 is sufficiently high. This condition is easily satisfied in vacuum devices and free-electron lasers. In a dense solid-state plasma one should take into account electron-electron interaction effects. Then one finds[13] that the strong coherent radiation is observed at the frequency,

$$\tilde{f} = \frac{v_0}{a_x} - f_p, \tag{3}$$

only if the velocity v_0 exceeds a *threshold* value,

$$v_0 > v_{th} \simeq f_p a_x = \sqrt{\frac{n_s e^2 a_x}{m^\star \epsilon}}; \tag{4}$$

for details see Ref. 13. Otherwise, at $v_0 \ll f_p a_x$, the electron system emits at the plasma frequency (2), just due to the heating of the system (the thermal radiation).

The condition (4) is of crucial importance for successful device operation. It is very difficult, if possible at all, to satisfy it in semiconductor structures. For example, in a GaAs quantum well with $m^\star = 0.067 m_0$, $\epsilon = 12.8$, $n_s \sim 3 \times 10^{11}$ cm^{-2}, and $a_x \sim 1$ μm the threshold velocity (4) is about 10^8 cm/s which is more than 4 times larger than the Fermi velocity at the same density.

In this paper we show that graphene, a recently discovered[14–16] one-monolayer-thin two-dimensional carbon allotrope, offers a great opportunity to realize the Smith-Purcell emitter. We propose a specific few-layer graphene-boron nitride structure which is shown to be able to emit electromagnetic radiation in the frequency range from ∼0.1 up to ∼30 THz with the power density up to 0.5 W/cm^2. This may become a new, very interesting application of graphene.

II. PROPOSED STRUCTURE AND ITS PARAMETERS

A. Qualitative discussion

The spectrum of electrons in graphene, in contrast to semiconductor systems, is linear:

$$E_\pm(\mathbf{p}) = \pm v_F \sqrt{p_x^2 + p_y^2}, \tag{5}$$

with the Fermi velocity $v_F \approx 10^8$ cm/s which is substantially higher than in semiconductors. As seen from the above discussion (Sec. I), in order to realize a solid-state Smith-Purcell emitter, the density of electrons should be low while the drift velocity should be large [Eq. (4)]. Figure 1 illustrates that this requirement is much easier to satisfy in graphene than in a system with the parabolic energy dispersion.

However, an attempt to directly apply the ideas of the Smith-Purcell emitter to graphene faces two difficulties. First, in graphene oscillations of the momentum do not lead to

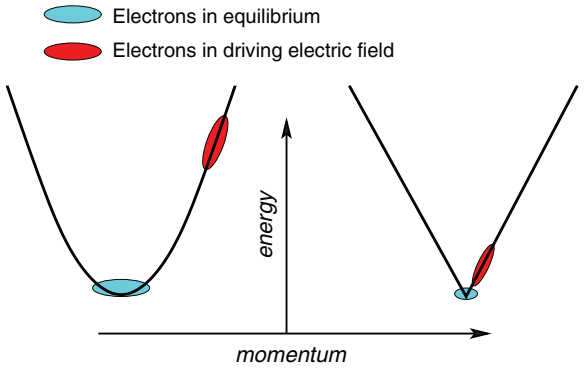

FIG. 1. (Color online) In order to accelerate a small amount of electrons up to velocities of order of $v_F \approx 10^8$ cm/s one needs a large change of the momentum in the case of the parabolic energy dispersion (semiconductors, left) and a much smaller change of the momentum in the case of the linear energy dispersion (graphene, right).

oscillations of the velocity and, hence, of the current, since the velocity $\mathbf{v}_\pm = \partial E_\pm(\mathbf{p})/\partial \mathbf{p}$ is not proportional to the momentum. Second, the condition $v_{th} < v_0 \leqslant v_F$ restricts the required electron density by the values of order of $n_s \simeq 10^{10}$ cm^{-2}. It is known, however, that due to internal inhomogeneities the average density of electrons in a graphene sheet typically exceeds $\simeq 10^{11}$ cm^{-2} even at the Dirac point.

B. Basic design

Both difficulties can be overcome by using, instead of continuous graphene layers, an array of narrow stripes of graphene. This leads to the following basic design of the emitter[17] (Fig. 2). The first (active) graphene layer lies on a substrate made out of a dielectric material, e.g., SiO_2 or hexagonal boron nitride (h-BN) [Fig. 2(a)]. This layer consists of an array of stripes with the width W_y and the period a_y and has two metallic contacts "source 1" and "drain 1" [Fig. 2(c)]. Above the first graphene sheet lies a thin dielectric layer, made out of a few monolayers of h-BN. A second graphene layer [Fig. 2(d)] has the shape of a grating with the stripe width W_x and the period a_x, oriented perpendicular to the stripes of the first layer and covers the whole structure. It has a metallic "gate" contact [Fig. 2(d)]. The side view of the whole structure is shown in Fig. 2(b).

Due to the finite width W_y of graphene stripes in the first layer, the p_y component of the momentum is quantized, $p_y \simeq \pi\hbar n/W_y$, and a gap is opened up in the graphene spectrum,

$$E_{\pm,n,p_x} = \pm\sqrt{\Delta_0^2 n^2 + v_F^2 p_x^2}, \tag{6}$$

Fig. 3(a). The value of the gap,

$$2\Delta_0 = 2\frac{\pi\hbar v_F}{W_y}, \tag{7}$$

is controlled by the stripe width W_y and can be as large as $\simeq$40 meV ($\simeq$500 K) if $W_y \simeq 0.1$ μm. Notice that we do not need here nanoribbons with the stripe width below $\sim$10 nm, therefore in such still macroscopic stripes there should be no complications related to the additional strong scattering at the nanoribbon edges. In the stripes the linear density of electrons n_e and holes n_h per unit length is determined by formulas,

$$n_e(\mu,T) = \frac{g_s g_v}{W_y}\sum_{n=1}^{\infty}\int_0^\infty \frac{dx}{1+\exp\frac{\sqrt{n^2+x^2}-\mu/\Delta_0}{T/\Delta_0}},$$
$$n_h(\mu,T) = n_e(-\mu,T), \tag{8}$$

where μ is the chemical potential, T is the temperature, and $g_s = g_v = 2$ are spin and valley degeneracies. As seen from Fig. 3(b), the total linear charge density $n_l = n_e + n_h$ is about $\sim 12/W_y$ at room temperature. At $W_y \simeq 0.1$ μm this gives $n_l \approx 1.2 \times 10^6$ cm^{-1}. If to choose the period of the structure in the first layer a_y bigger than 1.2 μm, the average surface density $n_s = n_l/a_y$ will be smaller than 10^{10} cm^{-2}. Thus, by choosing the stripe structure with a sufficiently large ratio a_y/W_y one can satisfy the threshold condition (4) not only at low but even at room temperature. This can also be seen from the expression,

$$\frac{v_{\rm th}}{v_F} = \sqrt{\frac{e^2}{\epsilon\hbar v_F}\frac{n_l W_y}{\pi}\frac{a_x}{a_y}}, \tag{9}$$

which should be smaller than unity [Eq. (9) follows from (4) if to replace $m^\star$ by Δ_0/v_F^2]. The first factor $e^2/\epsilon\hbar v_F$ here is of order unity. The second factor $n_l W_y$ depends on the temperature, Fig. 3(b), and is about 10 at room and about 1 at liquid nitrogen temperature. The last factor a_x/a_y can be made as small as desired by the corresponding choice of geometrical parameters of the structure.

C. Estimates of operating parameters

In the operation mode, Fig. 2(b), a large dc voltage V_{sd} is applied between the source and drain contacts of the first layer and a small dc (gate) voltage V_{12}—between the first and the second graphene layer. The source-drain voltage causes a dc current in the first-layer stripes flowing in the x direction. The corresponding drift velocity should lie in the window $v_{th} < v_0 < v_F$. If the drift velocity is about 6×10^7 cm/s and the grating period $a_x \simeq 0.2$ μm, the fundamental frequency of the emitter will be about 3 THz. Dependent on the parameters this frequency can be red- or blue-shifted. The radiation is linearly polarized in the direction of the dc current (x direction).

Let us estimate the emitted power. Under the action of the dc source-drain voltage electrons move with the constant (average) drift velocity v_0. A small gate voltage V_{12} applied between the first and the second graphene layers results in the periodic time-dependent modulation of the velocity, $v_x(t) = v_0 + v_1\cos(2\pi v_0 t/a_x)$. The modulation amplitude v_1 is controlled by the gate voltage V_{12} and can be varied between 0 and v_0. Assume that we have a 70% modulation of the drift velocity, i.e., $v_1 \simeq 4 \times 10^7$ cm/s. Then the amplitude of the ac electric current density is $j_1 \simeq e n_s v_1$, the electric and magnetic fields of the emitted wave (calculated from Maxwell equations) are $E_1 = H_1 \simeq 2\pi j_1/c$ and the intensity of the emitted radiation (the Poynting vector) $W_{\rm rad} = cE_1^2/4\pi$. At the electron density $n_s \simeq 10^{10}$ cm^{-2} this gives a very large radiation power of

$$W_{\rm rad} \simeq \frac{\pi}{c}(e n_s v_1)^2 \simeq 0.5\ \text{W/cm}^2. \tag{10}$$

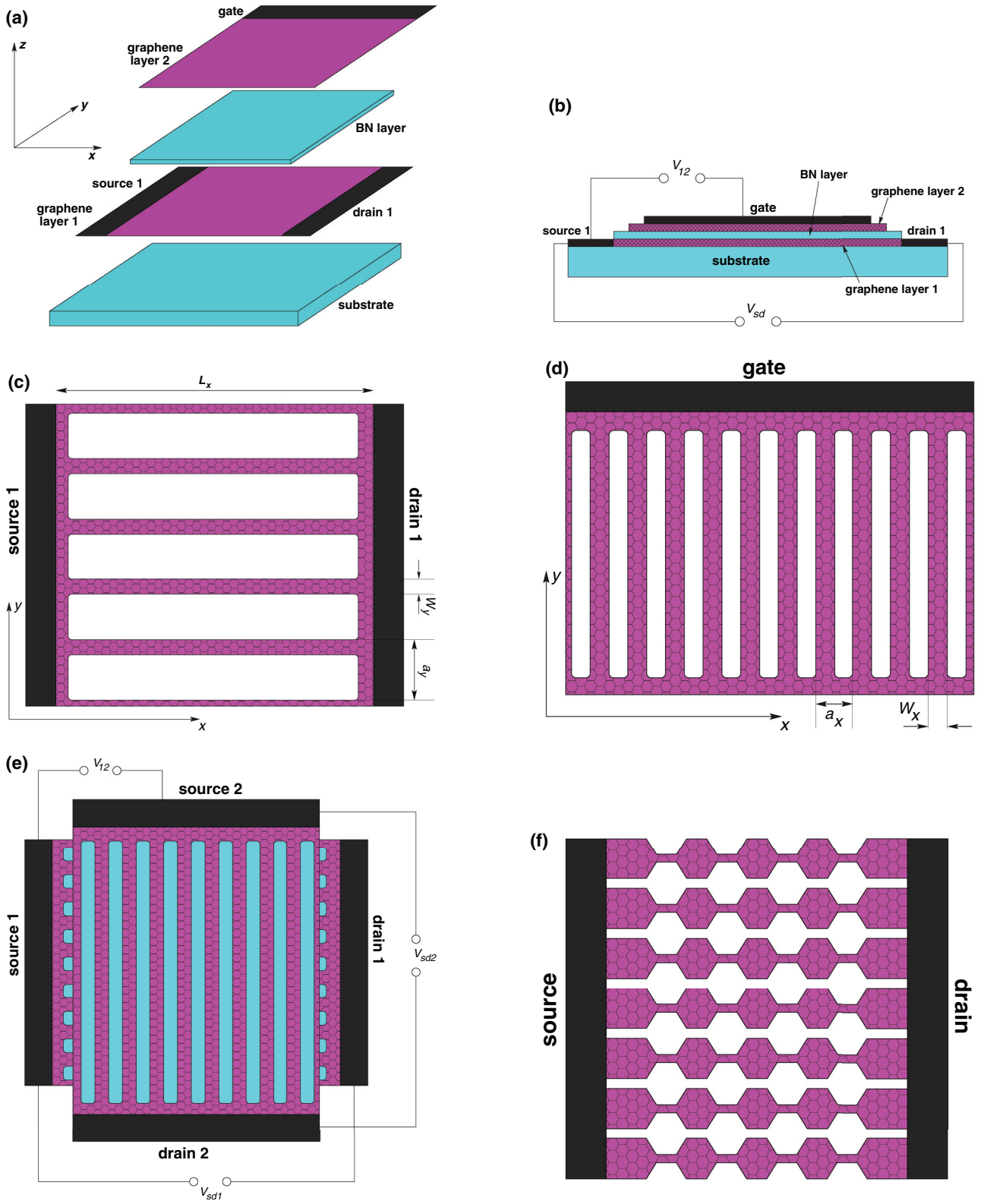

FIG. 2. (Color online) (a) The overall view of the device design. The first graphene layer lies on a substrate (made out of h-BN or SiO_2) and is covered by a few-nanometer thin h-BN dielectric layer. Two metallic contacts, "source 1" and "drain 1," are attached to the graphene layer 1 from the "west" and "east" sides. On top of the h-BN layer lies the second graphene layer with a metallic contact ("gate") attached on the "north" (or "south") side. (b) The side view of the graphene-based emitter. (c) The design of the first graphene layer. The central (operating) area of the layer is made in the form of a periodic array of narrow stripes. (d) The design of the second graphene layer (grating). (e) An alternative design of the top (grating) graphene layer with two contacts "source 2" and "drain 2." (f) A single-layer device structure with a modulated width of graphene stripes.

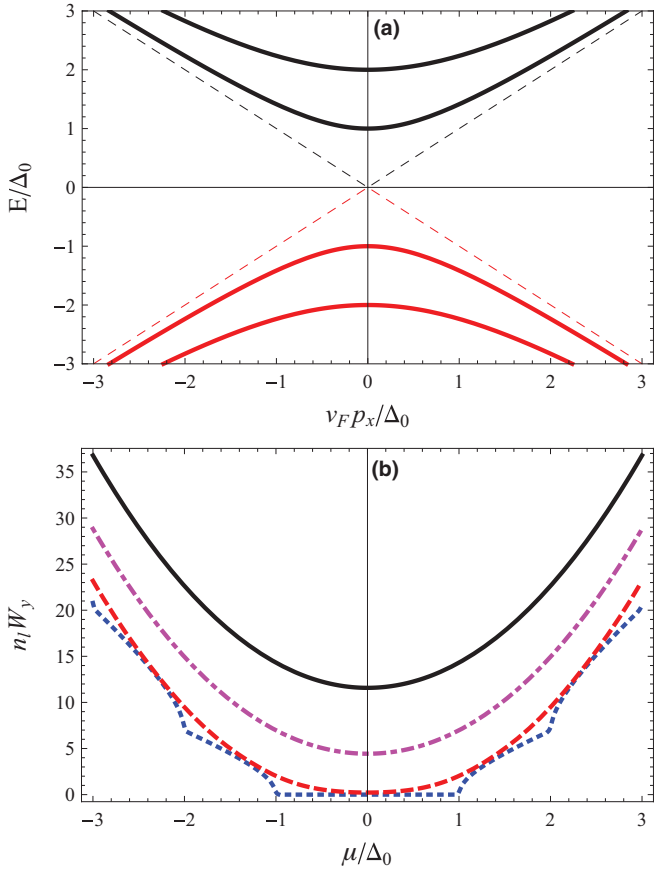

FIG. 3. (Color online) (a) The energy spectrum in the graphene stripes. If $W_y \simeq 0.1\ \mu$m, the gap $2\Delta_0$ is about 500 K. (b) The linear charge carrier density $n_l = n_e + n_h$ as a function of the chemical potential μ/Δ_0 at different values of the temperature: $T/\Delta_0 = 0.01$ (dotted, blue), 0.3 (dashed, red), 0.8 (dot-dashed, magenta), and 1.2 (solid, black). If $W_y \simeq 0.1\ \mu$m, the blue, red, magenta, and black curves approximately correspond to 2.5, 75, 200, and 300 K, respectively.

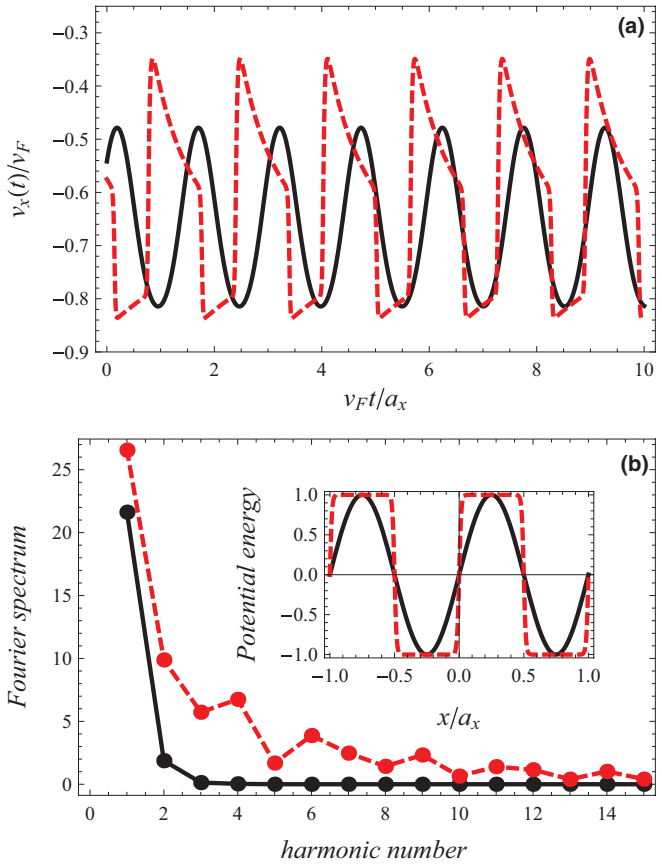

FIG. 4. (Color online) (a) The time dependence of the velocity $v(t)$ calculated for $U_0/\Delta_0 = 0.3$, $a_x\gamma/v_F = 1$, $eE_0a_x/\Delta_0 = 1$, and $S = 0.1$ (black solid curve) and $S = 10$ (red dashed curve). The average value of $v(t)/v_F$ in the cases $S = 0.1$ and $S = 10$ are 0.661 and 0.615, respectively. (b) The corresponding Fourier spectra. (Inset) The model periodic potential $U(x)$ (12) at $S = 0.1$ (black solid curve) and $S = 10$ (red dashed curve).

Estimating the Joule's heating power as $W_{\rm heat} \simeq j_0E_0 \simeq j_0^2/\sigma_{\rm min}$, where $\sigma_{\rm min} = 4e^2/h$ is the typical (minimal) conductivity of graphene,[15] we get

$$\frac{W_{\rm rad}}{W_{\rm heat}} \simeq \frac{\pi j_1^2/c}{j_0^2/\sigma_{\rm min}} \lesssim \frac{\pi\sigma_{\rm min}}{c} = 2\frac{e^2}{\hbar c}, \qquad (11)$$

i.e., the efficiency of the emitter is about $(1 \div 2)\%$ which is quite large for a tunable terahertz emitter and is comparable with the efficiency of free-electron lasers.[18] If the structure lies on a SiO_2 or BN 1-mm-thick substrate and the opposite side of the substrate is maintained at room temperature, the increase of temperature of the structure at $W_{\rm heat} \simeq 50$ W/cm^2 does not exceed 10–20 K, due to the very large surface-to-volume ratio in the two-dimensional graphene and to the high thermal conductivity of the substrate.

D. Harmonics generation

The proposed device may emit radiation not only at the fundamental frequency (1) but also at its harmonics. In the above discussion we have assumed that the periodic potential $U(x)$ produced by the voltage V_{12} between the two graphene layers has a simple sinusoidal form $U(x) = U_0\sin(2\pi x/a_x)$. This is a good approximation for the case when the distance D between the 2D electron layer and the grating is comparable with the grating period. In the proposed graphene-BN-graphene structure the thickness of the dielectric BN layer can be as small as a few nanometers while the grating period a_x is assumed to be larger than $\sim$0.1 μm. The ratio D/a_x is therefore much smaller than unity and the potential $U(x)$ has a steplike form; see inset in Fig. 4(b). The higher spatial harmonics will then lead to higher frequency harmonics in the emission spectrum. To show this quantitatively, we consider the motion of an electron with the spectrum (6) in a periodic potential $U(x)$ under the action of a strong dc electric field $E_0 = V_{sd}/L_x$ caused by the source-drain voltage; here L_x is the source-drain distance. Since the electron density must be kept low to avoid the influence of the plasma frequency [the condition (4)] we ignore the collective effects and describe the motion of electrons by single-particle equations. For the potential $U(x)$ we use a model expression,

$$U(x) = U_0\frac{\tanh[S\sin(2\pi x/a_x)]}{\tanh S}, \qquad (12)$$

with the amplitude U_0 and a steepness parameter S: If $S \lesssim 1$, the periodic potential is smooth and close to a single-harmonic sinusoidal form; if $S \gg 1$, it has a steplike form and contains many spatial Fourier harmonics [Fig. 4(b)]. The scattering of electrons by impurities and phonons is described by a phenomenological scattering rate $\gamma = 1/\tau$. Then equations to be solved assume the form,

$$\frac{dp_x}{dt} = -eE_0 - \gamma p_x - \frac{dU(x)}{dx}, \tag{13}$$

$$\frac{dx}{dt} = v_x = \frac{v_F^2 p_x}{\sqrt{\Delta_0^2 + v_F^2 p_x^2}}. \tag{14}$$

They contain two sources of nonlinearity: The nonsinusoidal periodic potential $U(x)$ and the graphene-specific nonlinear velocity-momentum relation.

Figure 4 shows results of the numerical solution of Eqs. (13) and (14) for parameters $U_0/\Delta_0 = 0.3$, $eE_0a_x/\Delta_0 = 1$, and $a_x\gamma/v_F = 1$. If $2\Delta_0 \simeq 500$ K $\simeq 40$ meV the first two numbers correspond to $U_0 \simeq 6$ meV and $E_0 \simeq 0.1$ V/μm for the grating period $a_x \simeq 0.2$ μm. The last number means that the mean free path is of order of the grating period ($\simeq$0.2 μm) and the voltage drop per period (and per the mean free path) is about 20 mV. All the required conditions can be experimentally realized. For example, in Ref. 19 a high-current regime has been studied in a graphene stripe of the width 350 nm under the action of a dc electric field up to $\sim$1.5 V/μm, i.e., more than one order of magnitude larger than we have assumed here. The mean free path measured in Ref. 20 was found to be about 1 μm at room temperature, which is five times bigger than was used in our calculations. Under the assumed conditions the emission of optical phonons[12]—the most "dangerous" channel of an inelastic electron scattering—is strongly suppressed since the voltage drop per the mean free path ($\simeq$20 mV) is much smaller than the optical phonon energy in graphene ($>$160 meV[12]).

Figures 4(a) and 4(b) show the time dependence of the velocity $v_x(t)$ and its Fourier spectra, respectively; the black (solid) and the red (dashed) curves correspond to the small ($S = 0.1$) and large ($S = 10$) values of the steepness parameter S. One sees that at $S \ll 1$ the current $j_x(t) = en_s v_x(t)$ has an almost sinusoidal form with the dominating first and substantially weaker second frequency harmonics. The average drift velocity for the chosen parameters is $v_0/v_F \approx 0.661$ which corresponds to the fundamental frequency (1) $f_1 = f \approx 0.661 v_F/a_x \simeq 0.66$–$3.3$ THz for $a_x \simeq 1$–0.2 μm. At $S \gg 1$ the time dependence of the current is strongly nonmonochromatic with quite large second, third, fourth, and even sixth frequency harmonics. The average drift velocity for the chosen parameters is $v_0/v_F \approx 0.615$ with the resulting fundamental frequency $f_1 = f \approx 0.615 v_F/a_x$. This corresponds, for the same values of the grating period $a_x \simeq 1 - 0.2$ μm, to the first harmonic $f_1 \simeq 0.6$–3 THz, second harmonic $f_2 \simeq 1.2$–6 THz, fourth harmonic $f_4 \simeq 2.4$–12 THz and so on. As seen from Fig. 4(b) even the ninth harmonic (f_9 is up to 27 THz) has the amplitude only one order of magnitude smaller than the first one.

E. Alternative embodiments

So far we have discussed the traditional field-effect-transistor-type design with the top graphene layer having only one (gate) contact [Fig. 2(d)]. Alternatively, the top layer may have two metallic contacts, "source 2" and "drain 2," which gives the opportunity to drive a dc current in the second layer, too [Fig. 2(e)]. Then the system becomes symmetric, with the second (first) layer serving as the grating coupler for the first (second) layer and the opportunity to emit radiation with both x and y polarization independently controlled by the source-drain voltages V_{sd1} and V_{sd2}. Another possible embodiment employing a single graphene layer is shown in Fig. 2(f). The periodic potential $U(x) \propto 1/W_y(x)$ is produced in this case by the alternating stripe width $W_y(x)$. An advantage of this design is that it employs only one graphene layer. The mean free path should exceed the grating period.

In addition to the ability to work as an emitter, the proposed device may also operate as a new type of a field-effect-transistor (amplifier) combined with a plane radiating antenna. Indeed, the intensity of the emitted radiation is determined by the amplitude of the ac electric current j_1. This amplitude depends, in its turn, on the voltage V_{12} between the first and second graphene layers: If $V_{12} = 0$, the current flowing from the source to the drain does not depend on time and no radiation is emitted; if $V_{12} \neq 0$, the current gets modulated and the device emits an electromagnetic signal. The radiation intensity can be very large [$\simeq$5 kilowatts from square meter; Eq. (10)] at the few-millivolt input signal V_{12} (see estimates above). The proposed device thus amplifies an input signal and emits it directly to the surrounding space within the same physical process.

The single-layer graphene absorbs only 2.3% of visible light.[21] The h-BN layer is a dielectric with a large band gap and is also transparent. The proposed powerful terahertz devices will therefore be very thin, light, and practically invisible. Furthermore, such few-nm-thick devices can be bent up focusing radiation and producing a huge concentration of THz power in a very small spatial volume.

III. CONCLUSIONS

To summarize, we have proposed a new type of few-atomic-layers-thin, light, bendable, almost invisible, and voltage-tunable graphene-based device and provided detailed estimates of all important operating parameters. The proposed structure is shown to be able to produce a powerful electromagnetic radiation in a broad range of terahertz frequencies.

ACKNOWLEDGMENTS

The author would like to thank Ulrich Eckern and Roland Grenz for interest in this work and Geoffrey Nash, Fabrizio Castellano, Jerome Faist, and Taiichi Otsuji for useful discussions. The research leading to these results has received funding from the Deutsche Forschungsgemeinschaft and the European Community's Seventh Framework Programme (FP7/2007-2013) under Grant No. 265114.

*sergey.mikhailov@physik.uni-augsburg.de

[1]S. J. Smith and E. M. Purcell, Phys. Rev. **92**, 1069 (1953).
[2]D. C. Tsui, E. Gornik, and R. A. Logan, Solid State Commun. **35**, 875 (1980).
[3]R. A. Höpfel, E. Vass, and E. Gornik, Phys. Rev. Lett. **49**, 1667 (1982).
[4]N. Okisu, Y. Sambe, and T. Kobayashi, Appl. Phys. Lett. **48**, 776 (1986).
[5]K. Hirakawa, K. Yamanaka, M. Grayson, and D. C. Tsui, Appl. Phys. Lett. **67**, 2326 (1995).
[6]M. Dyakonov and M. Shur, Phys. Rev. Lett. **71**, 2465 (1993).
[7]P. Bakshi, K. Kempa, A. Scorupsky, C. G. Du, G. Feng, R. Zobl, G. Strasser, C. Rauch, C. Pacher, K. Unterrainer, and E. Gornik, Appl. Phys. Lett. **75**, 1685 (1999).
[8]W. Knap, J. Lusakowski, T. Parenty, S. Bollaert, A. Cappy, V. V. Popov, and M. S. Shur, Appl. Phys. Lett. **84**, 2331 (2004).
[9]V. Ryzhii, A. Satou, M. Ryzhii, T. Otsuji, and M. S. Shur, J. Phys. Condens. Matter **20**, 384207 (2008).
[10]A. El Fatimy, N. Dyakonova, Y. Meziani, T. Otsuji, W. Knap, S. Vandenbrouk, K. Madjour, D. Théron, C. Gaquiere, M. A. Poisson, S. Delage, P. Prystawko, and C. Skierbiszewski, J. Appl. Phys. **107**, 024504 (2010).
[11]T. Otsuji, T. Watanabe, A. El Moutaouakil, H. Karasawa, T. Komori, A. Satou, T. Suemitsu, M. Suemitsu, E. Sano, W. Knap, and V. Ryzhii, J. Infrared Milli. Terahz. Waves **32**, 629 (2011).
[12]T. Otsuji, S. A. B. Tombet, A. Satou, H. Fukidome, M. Suemitsu, E. Sano, V. Popov, M. Ryzhii, and V. Ryzhii, J. Phys. D: Appl. Phys. **45**, 303001 (2012).
[13]S. A. Mikhailov, Phys. Rev. B **58**, 1517 (1998).
[14]K. S. Novoselov, A. K. Geim, S. V. Morozov, D. Jiang, Y. Zhang, S. V. Dubonos, I. V. Grigorieva, and A. A. Firsov, Science **306**, 666 (2004).
[15]K. S. Novoselov, A. K. Geim, S. V. Morozov, D. Jiang, M. I. Katsnelson, I. V. Grigorieva, S. V. Dubonos, and A. A. Firsov, Nature (London) **438**, 197 (2005).
[16]Y. Zhang, Y.-W. Tan, H. L. Stormer, and P. Kim, Nature (London) **438**, 201 (2005).
[17]S. A. Mikhailov, European patent pending, 2011.
[18]D. A. Jaroszynski, R. Prazeres, F. Glotin, J. M. Ortega, D. Oepts, A. F. G. van der Meer, G. M. H. Knippels, and P. W. van Amersfoort, Phys. Rev. Lett. **74**, 2224 (1995).
[19]A. Barreiro, M. Lazzeri, J. Moser, F. Mauri, and A. Bachtold, Phys. Rev. Lett. **103**, 076601 (2009).
[20]Z. Q. Li, E. A. Henriksen, Z. Jiang, Z. Hao, M. C. Martin, P. Kim, H. L. Stormer, and D. N. Basov, Nature Physics **4**, 532 (2008).
[21]R. R. Nair, P. Blake, A. N. Grigorenko, K. S. Novoselov, T. J. Booth, T. Stauber, N. M. R. Peres, and A. K. Geim, Science **320**, 1308 (2008).